13th World Conference on Earthquake Engineering
Vancouver, B.C., Canada
August 1-6, 2004
Paper No. 1146

MODIFIED SLIDING MODE CONTROL USING TARGET DERIVATIVE OF LYAPUNOV FUNCTION

Sang-Hyun Lee[1], Kyung-Won Min[2] and Hongjin Kim

SUMMARY

This paper presents a modified sliding mode control (SMC) algorithm for vibration control of structures to enhance the control performance of the widely-used SMC algorithm. In modified SMC, the control force is determined to meet conditions imposed on the target derivative of Lyapunov function. A shape function is developed to determine which one of the equivalent and corrective control, which are two terms comprising SMC, is a dominating part in controlling structures. Simulation results of show that the proposed method is able to enhance the performance for control of drifts, accelerations, and relative displacements. Moreover, it is observed that the performance is insensitive to the fundamental vibrating period and it utilizes the less control energy when compared to the original SMC.

INTRODUCTION

During last decades, significant scholastic efforts have been made for the development of active control devices and algorithms for large scale civil structures subjected to earthquake loads, and the effectiveness has been verified through extensive analytical and experimental studies [1-4]. For the practical application of the active control strategy to civil engineering, problem of stability and robustness is one of great issues and examined [5, 6]. A design of controller which guarantees the stability of nonlinear system as well as linear system, is possible using Lyapunov stability theory, which requires the definition of positive definite Lyapunov function, and the corresponding controller is designed to make the derivative of the Lyapunov function negative semi-definite [7-9]. Wu et al. proposed the modified bang-bang control by using Lyapunov's direct method [10]. Dyke et al. used magnetorheological (MR) damper designed to dissipate energy maximally by choosing the Lyapunov function as the total vibratory energy [11]. Min et al. proposed the probabilistic control algorithm, which determines the direction of a control force by Lyapunov controller design method [12], and Hwang et al. verified its efficiency through the experimental test [13]. The efficiency of the Lyapunov controller depends on the identification of the Lyapunov function.

Sliding mode control (SMC), one of the Lyapunov controllers, has been applied to the control of civil engineering structures under earthquake and wind loads, and its effectiveness and robustness were

1 Researcher, Research Institute of Engineering Science, Seoul National University, Shinlim-dong, Gwanak-gu, Seoul, Korea, e-mail: lshyun00@msn.com

2 Associate Professor, Department of Architectural Engineering, Dankook University, Seoul, Korea, e-mail: hongjinkim@cricmail.net

3 Visiting Assistant Professor, Dept. of Architectural Engineering, Dankook University, Seoul, Korea

verified through theoretical and experimental studies [14-18]. SMC determines the sliding surface where the motion of a structure is stable, and Lyapunov function is defined as a scalar function proportional to the distance of states to the sliding surface.

In SMC framework, the control force is given as the summation of a *corrective control force* and an *equivalent control force* [19]. The corrective control force makes the response trajectory deviated from the sliding surface back into the sliding surface while the equivalent control force causes the response to be parallel to the sliding surface or, in special case, keeps the trajectory staying in the sliding surface. The effectiveness and robustness of SMC depend on which one of above two forces is the dominating part of the control force, and the effect is strongly related to the dynamic characteristics of the sliding surface determined by the LQR method [20].

Based on the control objectives and capacity of actuator, sliding mode controller can be not only linear one which generates control force proportional to states or excitation signal, but also nonlinear one such as bang-bang controller which generates maximum force irrespective of magnitude of states or excitation. However, since SMC is generally designed to satisfy the condition that the derivative of Lyapunov function is just negative semi-definite, linear controllers by previous studies cannot make most of actuator and bang-bang controller generate unnecessary large control force.

In this paper, a concept of target derivative of Lyapunov function is proposed for determining the weighting between corrective and equivalent control parts. A shape function is developed for this purpose. This function plays a role similar to that of a saturation function of Lee et al. [21] or a shifted sigmoid function of Ertugrul et al. [22], which are developed to eliminate the chattering phenomenon which happens in Lyapunov controller such as SMC. Numerical simulations using single-degree-of-freedom (SDOF) and multi-degree-of-freedom (MDOF) systems under seismic excitations have been performed to evaluate the effectiveness of the proposed algorithm. Simulation results show that the proposed algorithm enhances the performance for control of drifts, inter-story drifts, and accelerations comparing to those by the original SMC.

DESIGN OF SLIDING MODE CONTROL

Equation of Motion

State-space form equation of an n-DOF second order mass-damping-spring system subjected to a ground acceleration $\ddot{x}_g$ and control force vector $\mathbf{u}$ of size $r\times 1$, is given by

$$\dot{\mathbf{z}} = \mathbf{A}\mathbf{z} + \mathbf{B}_1\ddot{x}_g + \mathbf{B}_2\mathbf{u} \tag{1}$$

where

$$\mathbf{z} = \begin{bmatrix} \mathbf{x} \\ \dot{\mathbf{x}} \end{bmatrix},\ \mathbf{A} = \begin{bmatrix} \mathbf{O} & \mathbf{I} \\ -\mathbf{M}^{-1}\mathbf{K} & -\mathbf{M}^{-1}\mathbf{C} \end{bmatrix},\ \mathbf{B}_1 = \begin{bmatrix} \mathbf{0} \\ \mathbf{M}^{-1}\mathbf{E} \end{bmatrix},\ \mathbf{B}_2 = \begin{bmatrix} \mathbf{0} \\ \mathbf{M}^{-1}\mathbf{H} \end{bmatrix} \tag{2}$$

and $\mathbf{M}$, $\mathbf{C}$, and $\mathbf{K}$ are, respectively, the mass, damping, and stiffness matrices of size $n\times n$, r is the number of controller, $\mathbf{x}$ is the displacement response vector of size $n\times 1$, and $\mathbf{E}$ and $\mathbf{H}$ are the earthquake influence and control force influence matrices, respectively. $\mathbf{I}$ and $\mathbf{0}$ are the identity and zero matrices, respectively.

Design of Sliding Surface

A sliding surface is given as a linear function of state vector $\mathbf{z}$ such that

$$\mathbf{s} = \mathbf{P}\mathbf{z} \tag{3}$$

in which $\mathbf{s}$ is a r-vector. The matrix $\mathbf{P}$ ($r\times 2n$) can be determined by a LQR method to minimize the following performance index [14].

$$J = \int_0^\infty \mathbf{z}^\mathbf{T}\mathbf{Q}\mathbf{z}\,dt \tag{4}$$

where $\mathbf{Q}$ is a $(2n\times 2n)$ positive definite weighting matrix.

Control Forces

A Lyapunov function V is selected as follows

$$V(\mathbf{s}) = 0.5\mathbf{s}^\mathbf{T}\mathbf{s} \tag{5}$$

The derivative of Lyapunov function is given as follows

$$\dot{V}(\mathbf{s}) = \boldsymbol{\lambda}(\mathbf{u}-\mathbf{u}_\mathbf{eq}) = \sum_{i=1}^{r}\dot{V}_i = \sum_{i=1}^{r}\lambda_i(u_i - u_{\mathrm{eq}i}) \tag{6}$$

where

$$\boldsymbol{\lambda} = \mathbf{s}^T\mathbf{P}\mathbf{B}_\mathbf{2} = [\lambda_1, \quad \lambda_2, \quad \ldots \quad \lambda_r] \tag{7}$$

$$\mathbf{u}_\mathrm{eq} = -(\mathbf{P}\mathbf{B}_\mathbf{2})^{-1}\mathbf{P}\mathbf{A}\mathbf{z} - (\mathbf{P}\mathbf{B}_\mathbf{2})^{-1}\mathbf{B}_\mathbf{1}\ddot{x}_g \tag{8}$$

Control force for $\dot{V}(\mathbf{s}) \le 0$ is expressed as a sum of equivalent control force $\mathbf{u}_\mathrm{eq}$ and corrective control force $\mathbf{u}_\mathrm{c}$ such that

$$\mathbf{u} = \mathbf{u}_\mathrm{eq} + \mathbf{u}_\mathrm{c} \tag{9}$$

in which $\mathbf{u}_\mathrm{c}$ is determined to satisfy the condition $\mathrm{sgn}(\boldsymbol{\lambda}\cdot\mathbf{u}_\mathrm{c}) \le 0$. $\mathrm{sgn}(\cdot)$ is a sign function.

Eq.(6) and Eq.(9) indicate that $\mathbf{u}_\mathrm{eq}$ makes the $\dot{V}(\mathbf{s})$ be zero and $\mathbf{u}_\mathrm{c}$ makes the $\dot{V}(\mathbf{s})$ be negative.

If control force is not applied, the $\dot{V}(\mathbf{s})$ becomes

$$\dot{V}(\mathbf{s}) = -\boldsymbol{\lambda}\mathbf{u}_\mathbf{eq} = \sum_{i=1}^{r}\dot{V}_{in} = -\sum_{i=1}^{r}\lambda_i u_{\mathrm{eq}i} \tag{10}$$

where subscript 'i' means the ith controller. It is noted that if $\dot{V}_{in} < 0$, the response trajectory approaches to the sliding surface without the help of the controller, which is reasonable since general civil engineering structures show stable behaviors without any controllers. If a designer hopes to realize an asymptotic stability using controller, i.e $\dot{V}(\mathbf{s}) \le 0$ at every instant, following continuous sliding mode controller (CSMC) can be designed [14].

$$\text{CSMC: } u_i^* = u_{\mathrm{eq}i} - \delta_i\lambda_i \tag{11}$$

in which $\delta_i \ge 0$, and $-\delta_i\lambda_i$ is the corrective force. The control force of Eq.(11) is linear one, and the corresponding $\dot{V}_i$ is

$$\dot{V}_i = -\delta_i\lambda_i^2 \tag{12}$$

Also, following discontinuous controllers are possible [14].

$$\text{SMC-I: } u_i^* = u_{\mathrm{eq}i} - \delta_i\,\mathrm{sgn}(\lambda_i)H(|\lambda_i| - \varepsilon_o) \tag{13}$$

$$\dot{V}_i = -\delta_i|\lambda_i|H(|\lambda_i| - \varepsilon_o) \tag{14}$$

$$\text{SMC-II: } u_i^* = \left[\begin{array}{ll} u_{\mathrm{eq}i} - \delta_i\,\mathrm{sgn}(\lambda_i)H(|\lambda_i| - \varepsilon_o); & if \quad \mathrm{sgn}(\lambda_i\cdot u_{\mathrm{eq}i}) < 0 \\ \qquad 0 & ; \; if \quad \mathrm{sgn}(\lambda_i\cdot u_{\mathrm{eq}i}) > 0 \end{array}\right. \tag{15}$$

$$\dot{V}_i = \left[\begin{array}{ll} -\delta_i|\lambda_i|H(|\lambda_i| - \varepsilon_o); & if \quad \mathrm{sgn}(\lambda_i\cdot u_{\mathrm{eq}i}) < 0 \\ \qquad -\lambda_i u_{\mathrm{eq}i} & ; \; if \quad \mathrm{sgn}(\lambda_i\cdot u_{\mathrm{eq}i}) > 0 \end{array}\right. \tag{16}$$

in which, $H(|\lambda|-\varepsilon_\mathrm{o})$ is the unit step function, and ε_o is the thickness of the boundary layer for eliminating chattering effect. $-\delta_i\,\mathrm{sgn}(\lambda_i)H(|\lambda_i| - \varepsilon_o)$ is the corrective force term.

SMC is generally designed to satisfy the condition that the derivative of Lyapunov function is just negative semi-definite. Eqs.(11), (13) and (15) indicate that each control force brings about the corresponding derivative of Lyapunov function, and this implies that control force is given if the derivative of Lyapunov function is specified to a certain value. The relative magnitude of $u_{\text{eq}i}$ becomes larger when $\dot{V}_i$ approaches to 0, while that of $u_{\text{c}i}$ becomes larger when $\dot{V}_i$ is getting smaller than 0. Lee at al. showed that the effectiveness of SMC depends on which one of the two forces is the dominating part of the control force, and that the effect is strongly related to the dynamic characteristics of the sliding surface determined by the LQR method[20]. Accordingly, the derivative of Lyapunov function used in SMC should be considered as a parameter which is specified by the designer.

Maximum Capacity of Control Actuator and Saturated Controller

For large-scale civil structures under seismic loads, it is almost impossible to realize the control force of Eq.(11), (13), and (15) which keeps the response trajectory to be always in the sliding surface since it requires substantially huge control forces equal to the seismic forces. Therefore, it is necessary to consider an actuator saturation problem in design of SMC when the controller capacity is less than the seismic force. The upper limit of control force, $\mathbf{u}_{\text{max}}$, is determined by the procedure proposed by Lee et al. [20]

$$\left| m_1^{-1} \boldsymbol{\varphi}^{\mathbf{T}} \mathbf{H} \mathbf{u}_{\text{max}} \right| = \rho \omega_o^2 S_d \left(\omega_o , \xi_o \right) \tag{17}$$

where $0 \le \rho \le 1$, $m_1 = \boldsymbol{\varphi}^{\mathbf{T}} \mathbf{M} \boldsymbol{\varphi}$, $\omega_o = \sqrt{\boldsymbol{\varphi}^{\mathbf{T}} \mathbf{K} \boldsymbol{\varphi} / \boldsymbol{\varphi}^{\mathbf{T}} \mathbf{M} \boldsymbol{\varphi}}$, $\xi_o = \boldsymbol{\varphi}^{\mathbf{T}} \mathbf{C} \boldsymbol{\varphi} / 2 \omega_o m_1$, and S_d and $\boldsymbol{\varphi}$ are, respectively, a displacement spectrum and a fundamental mode vector of the mass-damping-spring system. The Newmark design spectrum is used in this paper for obtaining a displacement spectrum [23].

With the $\mathbf{u}_{\text{max}}$ obtained by using the above method, the control forces in Eqs. (11), (13) and (15) are saturated as

$$u_i = \begin{cases} u_i^* ; & \text{if} \quad \left| u_i^* \right| < u_{i\,\text{max}} \\ u_{i\,\text{max}} \,\text{sgn}(u_i^*); & \text{if} \quad \left| u_i^* \right| > u_{i\,\text{max}} \end{cases} \tag{18}$$

MODIFIED SLIDING MODE CONTROL (MSMC)

In this section, a procedure is described in detail for modifying the sliding mode control in order that control performance is enhanced and insensitive to structural periods. A target derivative of Lyapunov function is proposed and control force is evaluated to meet the specified condition on the derivative of Lyapunov function. Shape function is developed for an efficient design of controller based on the distance of states from sliding surface. This shape function has another role of eliminating the chattering phenomena.

Target Derivative of Lyapunov Function

A design procedure for SMC is developed by setting a constraint condition on the derivative of Lyapunov function. In this paper, this condition is named as target derivative of Lyapunov function of *i*th controller denoted by $\dot{V}_{Ti}$. The underlying concepts are as follows;

1) $\dot{V}_{Ti}$, is assigned to be close to zero when the response trajectory approaches to the sliding surface. Then, the control force becomes close to u_{eq} and the states move along the sliding surface.

$$\lim_{|\lambda_i| \to 0} \dot{V}_{Ti} = 0 \tag{19}$$

2) $\dot{V}_{Ti}$ is set to be a function negatively proportional to the distance to the sliding surface, when the response trajectory deviates from the sliding surface. In this case, the magnitude of corrective force term

becomes large and the control force plays a role of making the response trajectory approach to the sliding surface.

$$\lim_{|\lambda_i|\to\infty} \dot{V}_{Ti} = -\kappa \left| \frac{\lambda_i}{\sigma_{\lambda_{io}}} \right|^q \tag{20}$$

in which q and κ are positive constants, and $\sigma_{\lambda_{io}}$ denotes the standard deviation of λ_{i0}, which is λ_i of uncontrolled system . The increase of the value of q brings about the rapid change of $\dot{V}_{Ti}$ with respect to λ_i .

Shape Function

To combine previous two concepts for $\dot{V}_T$ into one equation, following shape function is introduced.

$$S(\lambda_i) = \frac{\lambda_i^{2p}}{\lambda_i^{2p} + v^{2p}} \tag{21}$$

where p and v are natural number and they should be determined by designer. The shape function has following characteristics with respect to λ_i and plays a role similar to that of a saturation function or a shifted sigmoid function which was developed to eliminate the chattering phenomena.

$$\lim_{\lambda_i\to 0} S(\lambda_i) = 0 \tag{22}$$

$$\lim_{\lambda_i\to\infty} S(\lambda_i) = 1 \tag{23}$$

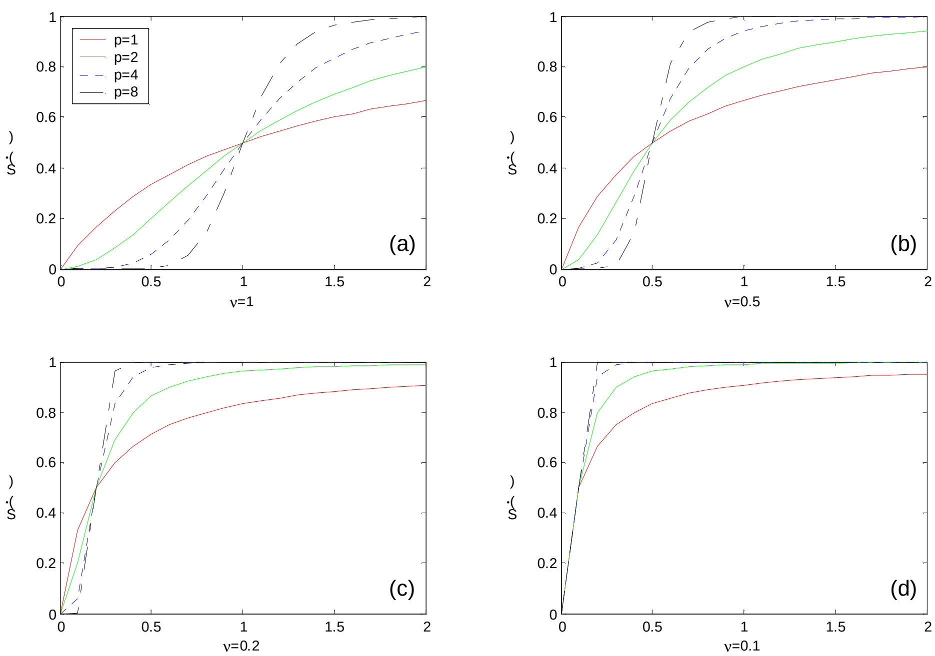

Figure 1 Variation of Function Shape Function

Figure 1 shows the plot of $S(\lambda_i)$ with respect to p and v. It can be known that increasing p makes $S(\lambda_i)$ to rapidly change between 0 and 1 with the change of $|\lambda_i|$. As v decreases, the region of $|\lambda_i|$ where $S(\lambda_i)$ is close to 0 decreases while the region of $|\lambda_i|$ where $S(\lambda_i)$ is close to 1 increases.

The target derivative can be rewritten with $S(\lambda_i)$ as

$$\dot{V}_{Ti} = -\kappa \frac{\lambda_i^{2p}}{\lambda_i^{2p} + v^{2p}} \left| \frac{\lambda_i}{\sigma_{\lambda_{io}}} \right|^q \tag{24}$$

Control Force by MSMC

The guidelines in designing MSMC using the target derivative concept are as follows; 1) Control is not required when the target derivative is achieved without the control force; 2) Only the necessary amount of the control force to achieve the target derivative is computed when it is in need; 3) Saturated controller is considered; The target derivative and its corresponding control force is given as

$$\dot{V} = \boldsymbol{\lambda}(\mathbf{u} - \mathbf{u_{eq}}) = \sum_i^r \lambda_i (u_i - u_{\mathrm{eq}i}) \le \sum_i^r \dot{V}_{Ti} \tag{25}$$

$$u_i^* = \begin{bmatrix} 0 & ; & \text{if } -\lambda_i u_{\mathrm{eq}i} \le \dot{V}_{Ti} \\ -\dot{V}_{Ti} / \lambda_i + u_{\mathrm{eq}i} & ; & \text{if } -\lambda_i u_{\mathrm{eq}i} > V_{Ti} \end{bmatrix} \tag{26}$$

$$u_i = \begin{bmatrix} u_i^* & ; & \text{if } \left|u_i^*\right| \le u_{i\max} \\ u_{i\max}\,\mathrm{sgn}\left(u_i^*\right) & ; & \text{if } \left|u_i^*\right| > u_{i\max} \end{bmatrix} \tag{27}$$

SIMULATION

The comparison between the performances of the SMC algorithms is made in this section. From the results of Yang's study [16], since the performances of CSMC, SMC-I, and SMC-II are generally equivalent, only CSMC is considered for the representative of the original SMC in this study. The NS acceleration component of El Centro earthquake (1940) with peak acceleration scaled to 0.112g is used as an earthquake load.

Evaluation Criteria

To evaluate the performance of controller in terms of the reduction of peak responses, the following evaluation criteria are considered.

$$J_1 = \max_{i=1,\ldots,n} \left\{ \frac{\max_t \left| x_i(t) \right|}{x^{\max}} \right\},\; J_2 = \max_{i=1,\ldots,n} \left\{ \frac{\max_t \left| d_i(t) \right|}{d_n^{\max}} \right\},\; J_3 = \max_{i=1,\ldots,n} \left\{ \frac{\max_t \left| \ddot{x}_{ai}(t) \right|}{\ddot{x}_a^{\max}} \right\} \tag{28}$$

in which $x_i(t)$ is the time history of the displacement of *i*th floor, and $x^{\max}$ is the uncontrolled maximum displacements for the first evaluation criterion, J_1, $d_i(t)$ is the time history of the interstory drift of the *i*th floor and $d_n^{\max} = \max_t \{d_i(t)\}$ is the uncontrolled maximum interstory drift for the second evaluation criterion, J_2, and $\ddot{x}_{ai}(t)$ is the time history of the absolute accelerations of the *i*th floor and $\ddot{x}_a^{\max}$ is the uncontrolled maximum absolute acceleration for the third evaluation criterion, J_3. The non-dimensionalized performance evaluation criteria, J_1, J_2, and J_3 measure the control performance for peak story drift, the peak inter-story drift, and peak acceleration, respectively. Another non-dimensionalized evaluation criterion, J_4, is used to measure the applied control energy

$$J_4 = \frac{\sqrt{\frac{1}{T} \sum_i^r \int_o^T u_i^2 dt}}{W} \tag{29}$$

in which *W* denotes the weight of structure and *T* is the duration time of control.

SDOF system

Simulations of SDOF systems with damping ratio, ξ_o, and natural period, T_n, were performed for the comparison of the performance of the proposed controllers. Mass=1ton, ξ_o =0.02 and T_n=0.5, 1.0, and 2 seconds are considered for simulation. u_{max} for each ρ is determined using Eq. (17). Sliding surface was obtained by the LQR method with a diagonal weighting matrix $\mathbf{Q} = \mathrm{diag}[\omega_n^2 \quad 1]$.

The forces by SMC do not always dissipate the structural energy since the defined Lyapunov function is not the structural energy, but the distance to the sliding surface. The sign of the control force dissipating the structural energy is always opposite to that of structural velocity [12]. Dyke et al. proposed a clipped optimal control law, which commands control signals only when control force dissipates the structural energy, and utilized it as a control algorithm for MR damper [24]. For the comparison and evaluation of the performance of MSMC for SDOF systems, the clipped control law is considered.

$$\text{CSMC-clipped}=\begin{cases} u; & if\ \mathrm{sgn}(u \cdot \dot{x}) < 0 \\ 0; & if\ \mathrm{sgn}(u \cdot \dot{x}) > 0 \end{cases} \tag{30}$$

The gain margin δ for CSMC and CSMC-clipped is $u_{\max} / \sigma_{\lambda_o}$. For MSMC, design parameters are determined as follows: $\kappa = 5 \cdot u_{\max} / \sigma_{\lambda_o}$; $\nu = 0.02\sigma_{\lambda_o}$; p=1. MSMC-I is the case for q= 2, and MSMC-II is the case for q=3.

Figure 2 shows the evaluation criteria according to ρ for the system with Tn=0.5 second. It is observed that the performance of all considered controller is enhanced with increasing ρ, implying that the performance level of SMC depends on the maximum control force limit because SMC requires generally large control force and thus causes saturation. It is also observed that MSMC provides the most significant reduction of both displacement (J_1 or J_2; J_1 and J_2 have the same vale for SDOF system) and absolute acceleration (J_3) responses at the same ρ. Furthermore, the control energies, J_4, by MSMC are smaller than that of the original CSMC. CSMC-clipped, which are designed to remove the undesirable effect that control force do not dissipate structural energy, enhances the performance of the original SMC, but its performance is inferior to that of MSMC.

It is shown that the values of evaluation criteria, J_1 and J_3, by MSMC-II is larger than that by MSMC-I for ρ>0.5. The reason why the performance of MSMC-II deteriorate when compared with that of MSMC-I for larger ρ, is that MSMC-II bring abut the rapid change of control force due to larger q, and this amplifies the ill effects particularly when the control force can be large due to larger ρ.

Figure 3 and 4 present the evaluation criteria for T_n=1.0 second, and T_n=2.0 second, respectively. The global variation trends are similar to that for T_n=0.5 second. It is observed that MSMC provides the most excellent performance in spite of the less used control energy.

MDOF System

For MDOF systems, the performance index is expressed as with the weighting matrix **Q** consisting of elements, q_{pi} and q_{ki} [20].

$$J = \int_o^{\infty} \left(\sum_i^n \frac{1}{2} q_{pi} k_i d_i^2 + \sum_i^n \frac{1}{2} q_{ki} m_i \dot{x}_i^2 \right) dt \tag{31}$$

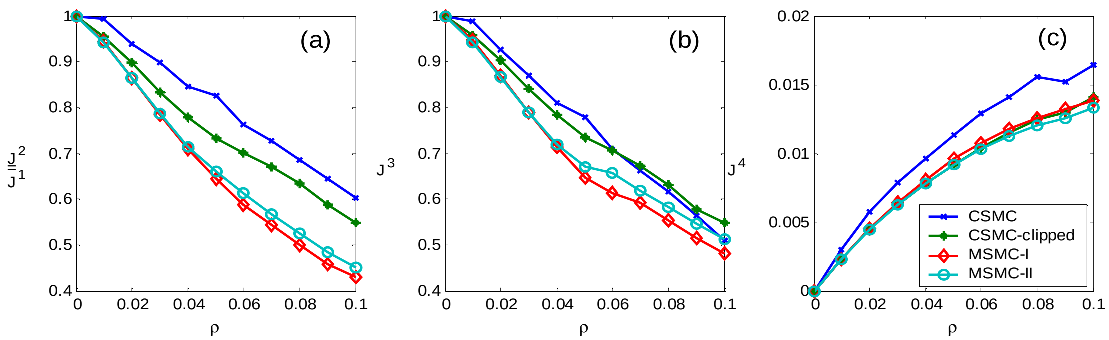

Figure 2. Performance evaluation criteria for T_n=0.5 second

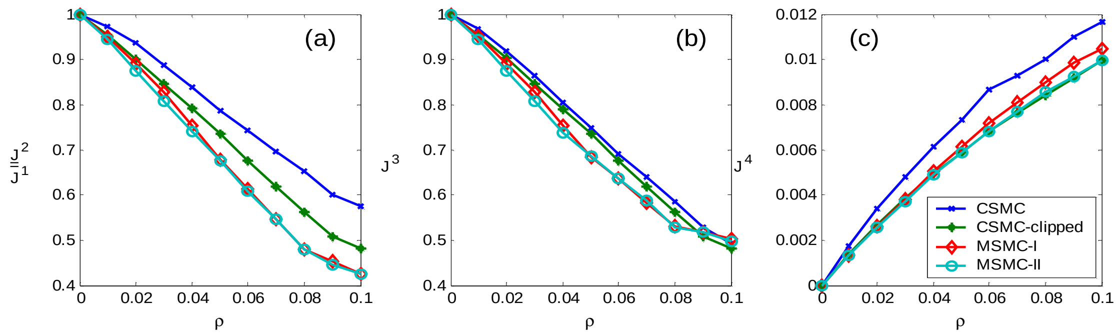

Figure 3. Performance evaluation criteria for T_n=1

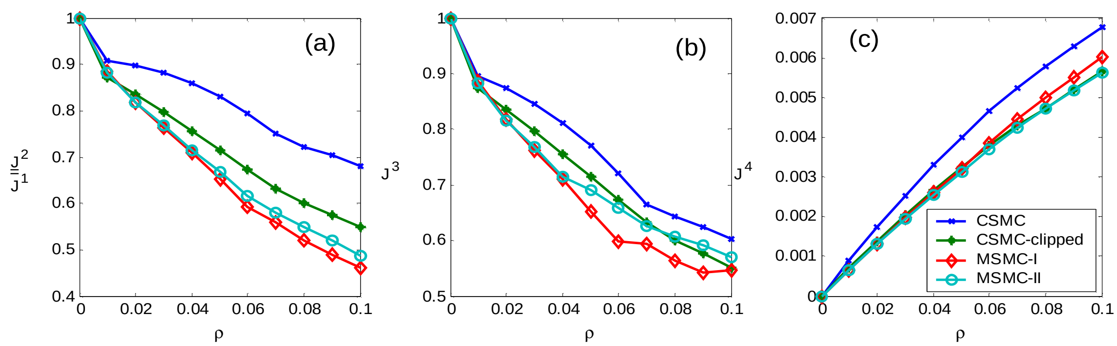

Figure 4. Performance evaluation criteria for T_n=2 second.

where k_i and m_i denote, respectively, stiffness and mass of ith story, and d_i and $\dot{x}_i$ denote ith interstory drift and relative velocity of ith floor to ground, respectively.

Example 1 – a three-story building with active bracing system (ABS)

A three-story building, which was studied as model structure for control by Yang et al. [16], is considered for example 1 of MDOF system. Every story has identical structural properties. The mass, stiffness, and damping coefficients are 1 ton, 980kN/m, and 1.407kNs/m, respectively. The fundamental period of the model structure is 0.45second. This building model with an active bracing system in the first story unit was studied by Yang et al. [16], who formulated the state-space equation in terms of inter- story displacements, d_i, and inter-story velocities, $\dot{d}_i$, and the weighting matrix **Q**=diag[10^5 10^4 10^3 1 1 1]. Lee et al. [20] determined the weighting matrix in Eq.(31) with $q_{k2}=q_{k3}=q_{p2}=q_{p3}=1$,and $q_{p1}=q_{k1}=100$, and compared the performances of the corresponding SMC algorithms. In this study, MSMC logic is applied to enhance the original CSMC with weighting matrices by Yang and Lee, which are denoted in Figure 5 by CSMC-$\mathbf{Q}_1$ and CSMC-$\mathbf{Q}_2$, respectively. δ =50 kN·kg·cm/s is used for CSMC and following design parameters are used for MSMC: $\kappa = 5 \cdot u_{\max} / \sigma_{\lambda_o}$; $\nu = 0.02\sigma_{\lambda_o}$; p=1; q=2. The NS acceleration component of El Centro earthquake (1940) with peak acceleration scaled to 0.112g is used as an earthquake load.

Figure 5 presents the evaluation criteria with respect to ρ . It also observed like the cases of SDOF systems that increasing ρ enhances the performance of every SMC algorithm. It is observed from Figure 5(a)-(c)

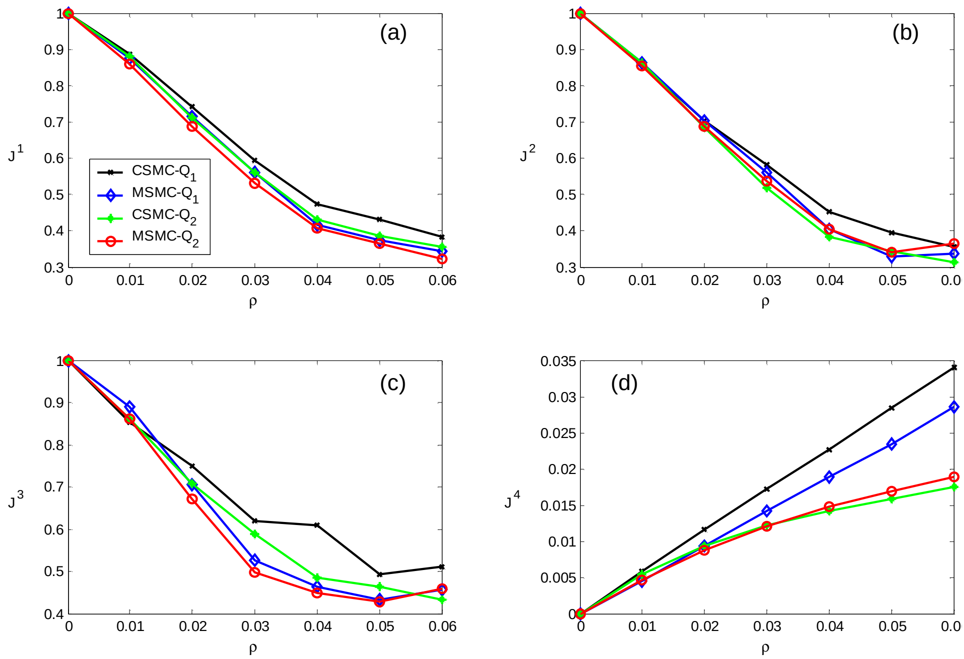

Figure 5. Performance evaluation criteria of 3-story building with an ABS

that the performance of MSMC-$\mathbf{Q}_1$ is superior to that of CSMC-$\mathbf{Q}_1$, and the performance of MSMC-$\mathbf{Q}_2$ is

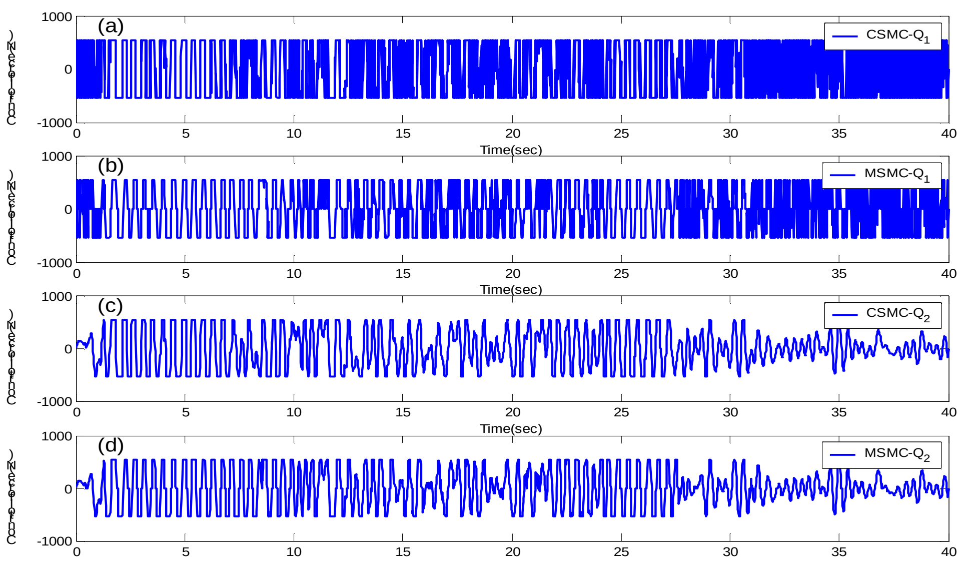

Figure 6. Control force when ρ =0.03

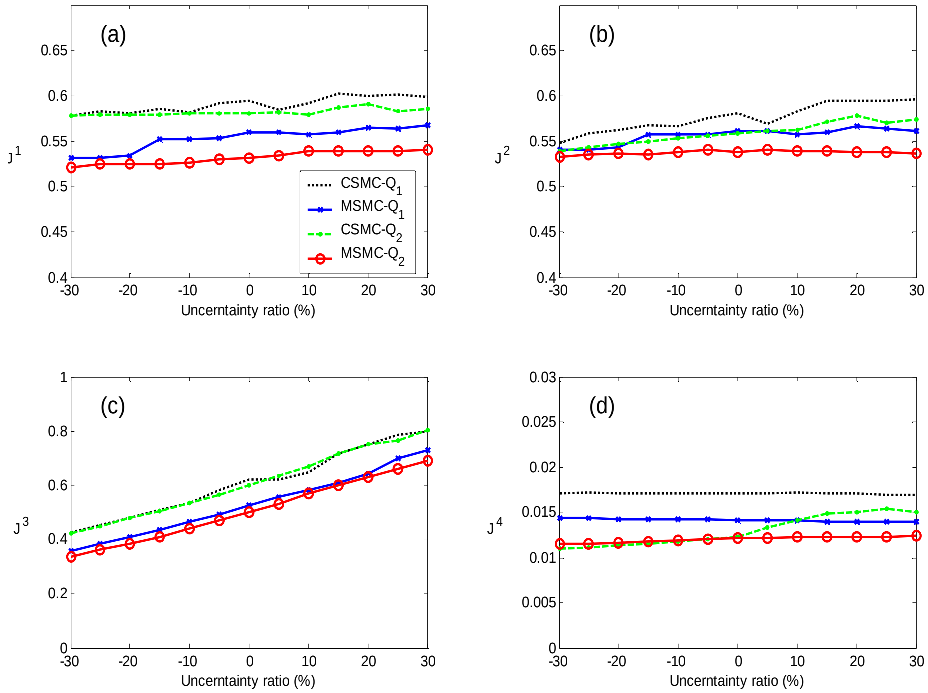

Figure 7. Performance evaluation criteria with uncertainties in stiffness

superior to that of CSMC-$\mathbf{Q}_2$. This fact indicates that MSMC logic can be used for enhancing the performance of the original SMC designed by specified weighting matrix. The controllers designed by $\mathbf{Q}_2$ provides more reduction of evaluation criteria than those designed by $\mathbf{Q}_1$, and furthermore Figure 5(d) informs that the controllers designed by $\mathbf{Q}_2$ uses less control energy than those designed by $\mathbf{Q}_1$. Figure 6 shows the time history of the control forces when ρ =0.03. It is evident that the undesirable chattering effects are remarkably reduced by using $\mathbf{Q}_2$ compared with the controllers using $\mathbf{Q}_1$. The RMS values of control forces are, respectively, 504N, 415N, 361N, and 356N for CSMC- $\mathbf{Q}_1$, MSMC- $\mathbf{Q}_1$, CSMC- $\mathbf{Q}_2$, and MSMC- $\mathbf{Q}_2$.

Even though the controller is well designed to show good performance for the model structure, if there is much discrepancy between the model structure and real structure, the control efficiency can deteriorate. Robustness of the control algorithm should be investigated according to the variation of the structural properties such as stiffness and mass. In this study, the robustness of the CSMC and MSMC is investigated with uncertainties in stiffness matrix. The range of uncertainty is from -30% to +30% of the original stiffness. Figure 7 shows the results from robustness investigation. u_{max} is determined with ρ =0.03. It is observed that all considered controllers have robust features in reducing displacement and inter-story drifts, and the performance of MSMC is most excellent in spite of the uncertainties in stiffness. It is noted that the acceleration response increases with the positive uncertainties in stiffness. This implies that the overestimation of the stiffness can bring about the increase of acceleration response.

Example 2 – a three-story building with an active mass damper (AMD)

The three-story building used in previous section, but with an AMD at the top story is studied in this section. The weighting matrix is chosen as with $q_{p1}=q_{p2}=q_{k1}=q_{k2}=1$,and $q_{p3}=q_{k3}=100$. The gain margin δ for CSMC is determined using $u_{\max}/\sigma_{\lambda_o}$, and $\kappa = 2u_{\max}/\sigma_{\lambda_o}$, $\nu = 0.1\sigma_{\lambda_o}$. p=1 and q=2 are used for MSMC.

As investigated in the example 1, the results shown in Figure 8 indicate that MSMC improve the performance of the original SMC in reducing the displacement, interstory drift, and absolute acceleration responses. Furthermore, the consumed control energy by MSMC is less than that by CSMC.

Example 3 – 20-story shear building

A 20-story shear building with an AMD at the top floor, which has the structural properties listed in Table 1, is used as an example of a long period MDOF structure. The natural vibrating period is 2.85 second. The weighting matrix is determined by using Eq.(31) with $q_{pi}=q_{ki}=1$ (i=1,…,19) and $q_{p20}=q_{k20}=100$. The gain margin δ for CSMC is determined using $u_{\max}/\sigma_{\lambda_o}$, $\kappa = 10u_{\max}/\sigma_{\lambda_o}$ and $\nu = 0.08\sigma_{\lambda_o}$. p=8 and q=3 are used for MSMC.

Figure 9 presents the evaluation with respect to ρ. It is obviously illustrated that the performance of MSMC is superior to that of CSMC in spite of the fact that MSMC utilizes less control energy than CSMC.

Figure 10 shows the time histories of the displacement and acceleration responses of the top floor when ρ =0.1. CSMC and MSMC reduce the peak value of the top floor displacement, which is 15.56cm when no control force is applied, to 8.89cm, and 7.13cm, respectively. The peak absolute acceleration response by CSMC and MSMC are, respectively, 1.52m/s^2 and 1.47m/s^2 while it is 2.08 m/s^2 without control. The CSMC is more effective for reducing the displacement response than the absolute acceleration response. Since CSMC utilizes the large control force and the sign of the control force changes rapidly when the response trajectory crossing the sliding surface, this performance deterioration of the CSMC for acceleration control occurs.

Floor	Story Mass	Story Stiffness	Natural Period	Damping Ratio
1, 2, 3, 4, 5	50(ton)	60000(kN/m)	T_1=2.75 second T_2=1.04 second T_3=0.63 second	2 %
6, 7, 8, 9, 10		45000(kN/m)		
11, 12, 13, 14, 15		30000(kN/m)		
16, 17, 18, 19, 20		21000(kN/m)		

Table 1. Structural properties of 20-story shear building

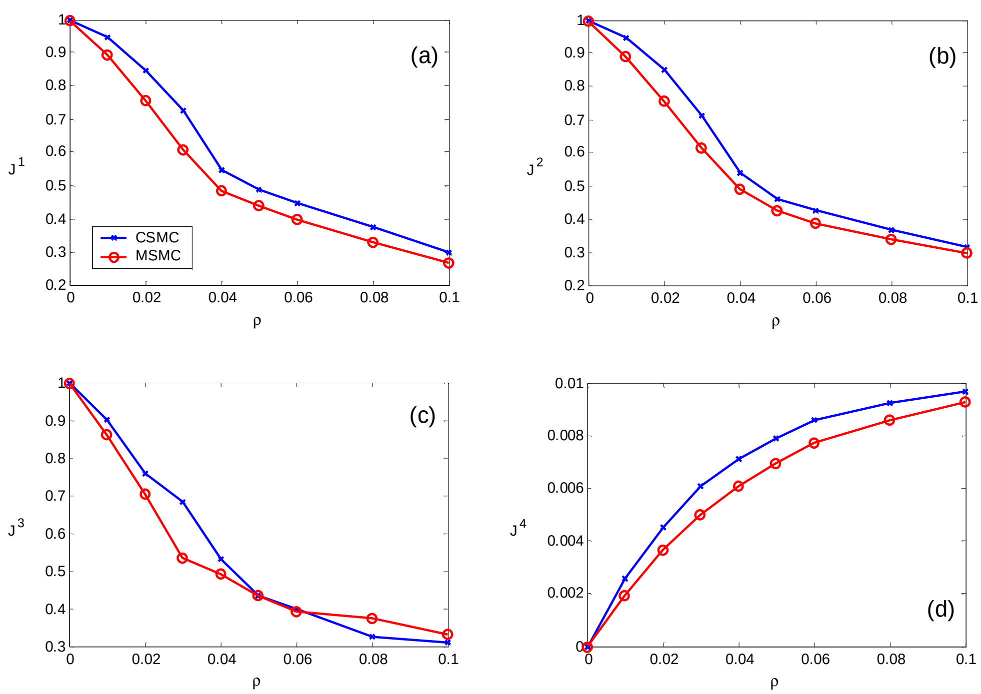

Figure 8. Performance evaluation of 3-story building with an AMD

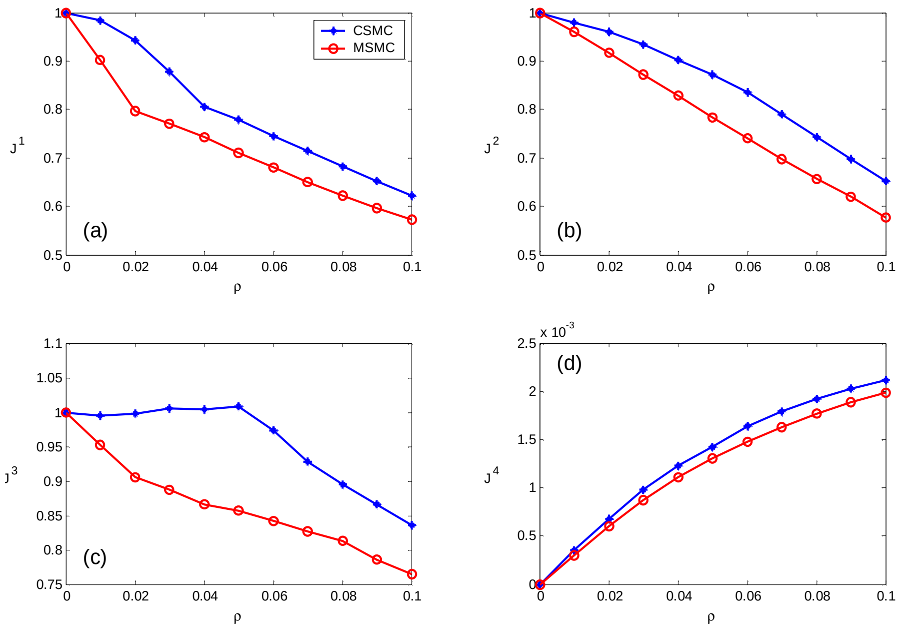

Figure 9. Performance evaluation of 20-story shear building with an AMD

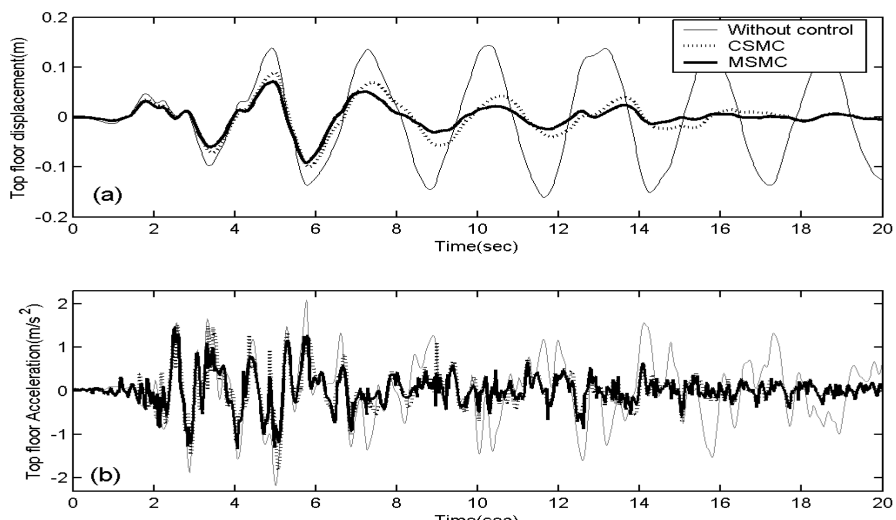

Figure 10. Time histories of the displacement and absolute acceleration at top floor of 20-story shear building with an AMD

CONCLUSION

In this study, a

modified SMC algorithm for vibration control of structures is proposed to enhance the control performance of the original SMC algorithm. A shape function is developed to determine which one of the equivalent and corrective control forces is a dominating part. This function also has a role of eliminating a chattering phenomenon, which is known to be a problem of Lyapunov controller such as SMC. Numerical simulations are performed to demonstrate the effectiveness of the proposed modified SMC algorithm using SDOF and MDOF systems under seismic excitations. The control performance depending on the limits of control force is also evaluated expressing the control force limits as a ratio of the seismic force, which is obtained directly from a Newmark design spectrum. Simulation results show that the proposed method is able to enhance the performance for control of the drifts, accelerations, and relative displacements over the original SMC. Moreover, it is observed that the performance of the proposed control algorithm is insensitive to the fundamental vibrating period and it utilizes the less control energy when compared to the original SMC.

ACKNOWLEDGEMENT

The authors would like to acknowledge the financial support from Korea Science and Engineering Foundation (KOSEF, Project No. R01-2003-000-11584-0).

REFERENCES

1. Soong TT. “Active Structural Control: Theory and Practic”e, Longman Wiley, London, 1990.
2. Reinhorn A M, Soong TT, Lin RC, Rilet M A, Wang Y P, Aizawa S, Higashino M. “Active Bracing System: A Full Scale Implementation of Active Control”, Technical Report NCEER-92-0020, State University of New York at Buffalo, Buffalo, NY, 1992.
3. Spencer BF Jr., Dyke SJ, Deoskar HS. “Benchmark problems in structural control: part I-active mass driver system”, Earthquake Engineering and Structural Dynamics, 1998. 27:1125-1139.
4. Chung LL, Lin RC, Soong TT, Reinhorn AM. “Experimental Study of Active Control for MDOF seismic Structures”, Journal of Engineering Mechanics, ASCE, 1989, 115(8):1609-1627.
5. Burl JB, “Linear Optimal Control: H_2 and $H\infty$ Methods”, Addison-Wesley, California, 1999.
6. Kemin Z. “Essentials of robust control, Prentice-Hall International”, New Jersey, 1998.
7. Junkins JL, Kim YD. “Introduction to Dynamics and Control of Flexible Structure”, AIAA, Inc. Washington, 1993.
8. Brogan WL. “Modern Control Theory, Prentice Hall”, Englewood Cliffs, New Jersey, 1991.
9. Slotine JJ, Li W. “Applied Nonlinear Contro”l, Prentice-Hall, Englewood Cliff, NJ, 1991.
10. Wu Z, Soong TT. “Modified bang-bang control law for structural control implementation”, ASCE, Journal of Engineering Mechanics, 1996, 122(8):771-777.
11. Dyke SJ, Spencer BF Jr, Sain MK, Carlson JD. An Experimental Study of MR Dampers for Seismic Protection, *Smart Material and Structures: Special Issue on Large Civil Structures*, 1998, 7:693-703.
12. Min KW, Hwang JS, Lee SH, Chung L. Probabilistic Approch for Active Control Based on Structural Energy, *Earthquake Engineering & Structural Dynamics*, 2003, 32(15):2301-2318.
13. Hwang JS, Min KW, Lee SH, Kim H, Chung L. Probabilistic Approch for Active Control Based on Structural Energy: Experimental Verification, *Earthquake Engineering & Structural Dynamics*, 2003, submitted.
14. Cai GP, Huang JZ, Sun F, Wang C. Modified Sliding-Mode Bang-Bang Control for Seismically Excited Linear Structures, *Earthquake Engineering and Structural Dynamics*, 2000, 29(11):1647-1657.
15. Kim SB, Yun CB. Sliding mode fuzzy control: Theory and verification on a benchmark structure, *Earthquake Engineering & Structural Dynamics*, 2000, 29:1587-1608.
16. Yang J N, Wu JC, Agrawal AK, Li Z. Sliding Mode Control for Seismic-excited Linear and Nonlinear Civil Engineering Structures, *Technical Report NCEER-95-0017*, National Center for Earthquake Engineering Research, 1994.

17. Yang JN, Wu JC, Agrawal AK. Sliding Mode Control for Seismically Excited Linear Structures", *Journal of Engineering Mechanics*, ASCE, 1995, 121:1386-1390.
18. Yang JN, Wu JC, Agrawal AK. Sliding Mode Control for Nonlinear and Hysteretic Structures, *Journal of Engineering Mechanics*, ASCE, 1995, 121:1330-1339.
19. Ertugrul M, Kaynak O. Neuro sliding mode control of robotic manipulators, *Journal of Engineering Mechanics*, ASCE, 2000, 10:239-263.
20. Lee SH, Min KW, Lee YC, Chung L. Improved Design of Sliding Mode Control for Civil Structures with Saturation Problem, *Earthquake Engineering & Structural Dynamics*, 2003, submitted.
21. Lee H, Kim E, Kang H, Park M. A new sliding-mode control with fuzzy boundary layer, *Fuzzy Set and System*, 2001, 120:135-143.
22. Ertugrul M, Kaynak. Neuro-sliding mode control of robotic manipulatiors, Mechatronics, 2000, 10:239-263.
23. Chopra AK. *Dynamics of Structures: Theory and Applications to Earthquake Engineering*, Prentice-Hall Inc., NJ, 2001.
24. Dyke SJ, Spencer, Spencer BF Jr, Sain MK, Carison JD. Modeling and control of magnetorheological dampers for seismic response reduction, *Smart Material and Structures*, 1996, 5:565-575.